Modern Physics Letters B, Vol. 25, No. 24 (2011) 1949–1961

DOI: 10.1142/S0217984911027194

World Scientific
www.worldscientific.com

STRUCTURAL AND MAGNETOELASTIC PROPERTIES OF $Y_3Fe_{27.2}Cr_{1.8}$ AND $Ce_3Fe_{25}Cr_4$ FERROMAGNETIC COMPOUNDS

N. TAJABOR*, A. GHOLIZADEH and M. BEHDANI

Department of Physics, Faculty of Sciences,
Ferdowsi University of Mashhad, Mashhad, Iran
**ntajabor@yahoo.com*

D. SANAVI KHOSHNOUD

Department of Physics, Faculty of Sciences, Semnan University, Semnan, Iran

H. SALAMATI

Faculty of Physics, Isfahan University of Technology, Isfahan 84156-83111, Iran

F. POURARIAN

Department of Material Science and Engineering,
Carnegie Mellon University, Pittsburgh, PA 15213, USA

Received 12 January 2011
Revised 12 May 2011

The structural and magnetoelastic properties of polycrystalline samples of $Y_3Fe_{27.2}Cr_{1.8}$ and $Ce_3Fe_{25}Cr_4$ intermetallic compounds are investigated by means of X-ray diffraction, thermomagnetic, thermal expansion and magnetostriction measurements in the temperature range of 77–500 K under applied magnetic fields up to 1.5 T. The well defined anomalies observed in the linear thermal expansion coefficient curves are associated with the magnetic phase transitions and presence of small amounts of 1:12 phase in the $Ce_3Fe_{25}Cr_4$ sample; the latter is also confirmed by AC susceptibility measurements. For $Y_3Fe_{27.2}Cr_{1.8}$, saturation behavior is observed in the anisotropic magnetostriction isotherms near the magnetic ordering temperature (T_C), whereas for $Ce_3Fe_{25}Cr_4$ compound, saturation starts well below T_C. The additional anomalies observed in the volume magnetostriction isotherms of both compounds are explained based on the anisotropy field in the a–b plane and along the c-axis of the unit cell.

Keywords: Intermetallic compounds; thermal expansion; magnetostriction; AC susceptibility.

PACS Number(s): 75.80.+q, 75.30.Gw

*Corresponding author.

1. Introduction

In searching for novel R-Fe (R = rare-earth) compounds, suitable for hard magnet applications, it was found that introduction of small amount of a stabilizing element M leads to the formation of a new series which may not exist in the binary phase diagram. This is the case for $R_3(Fe, M)_{29}$ compounds which exist for R = Ce, Pr, Nd, Sm, Gd, Tb, Dy and Y and M = Ti, V, Cr, Mn and Mo.[1–8]

This class of compounds has $Nd_3(Fe, Ti)_{29}$ stoichiometry with monoclinic symmetry and A2/m space group.[9] The $Nd_3(Fe, Ti)_{29}$-type structure is an intermediate between the rhombohedral Th_2Zn_{17}-type and tetragonal $ThMn_{12}$-type structures with two nonequivalent sites 2a, and 4i for R atoms and 11 nonequivalent sites for Fe/M atoms. The dominant crystal field parameter A_{20}, which determines the R sublattice anisotropy has opposite signs at the two nonequivalent sites of R atoms: at the 2a site with 1:12 like environment $A_{20} > 0$, and at the 4i site with 2:17 like environment $A_{20} < 0$. The product of second order Stevens coefficient (α_j) and A_{20} should be positive for axial anisotropy. In $R_3(Fe, M)_{29}$ compounds, the coupling of light (heavy) R atoms and Fe moments at 4.2 K are ferromagnetic (ferrimagnetic).[3]

The structure and magnetic properties of $R_3(Fe, Cr)_{29}Xn$ (R = Ce, Pr, Nd, Sm, Gd, Tb, Dy and Y and X = H, N, C) have also been studied.[1–7] The lattice constants and unit cell volume of $R_3(Fe, Cr)_{29}$ series decrease as the rare-earth atomic number increases from R = Pr to Dy (except for Ce) due to the lanthanide contraction. The Curie temperature variation across the rare-earth series shows the familiar behavior with a maximum at R = Gd. The Curie temperature for $Y_3Fe_{27.2}Cr_{1.8}$ is reported to be 427 K,[4] and for $Ce_3Fe_{25}Cr_4$ between 296 K (see Refs. 1 and 2) and 317 K.[3] In each series of $R_3(Fe, Cr)_{29}$, the saturation magnetization at 4.2 K decreases gradually from R = Nd to Dy, except for Ce. Hydrogenation, carbonation and nitrogenation of these compounds lead to a relative volume expansion of the unit cell, an increase in the Curie temperature, and a corresponding increase in the saturation magnetization at room temperature.[2,4,5] In the series of $R_3(Fe, Cr)_{29}$, the spin re-orientation transition of the easy magnetization direction is reported only for R = Nd and Tb.[3] But, such a transition has been observed in other 3:29 compounds, such as $(Sm_{1-x}Pr_x)_3Fe_{27.5}Ti_{1.5}$,[10] $Tb_3(Fe_{1-x}Co_x)_{27.4}V_{1.6}$,[11] $Tb_3(Fe, Ti)_{29}$ (see Ref. 12) and $R_3Fe_{29-x}V_x$ (R = Nd, Sm, and Tb).[3]

Since the Y element in $Y_3Fe_{27.2}Cr_{1.8}$ has no magnetic moment, the magnetostriction and thermal expansion of this compound can be used as a reference for exploring the contribution of the R elements to the magnetoelastic properties of the $R_3(Fe, Cr)_{29}$ compounds. The structural and magnetic parameters of the $R_3(Fe, Cr)_{29}$ compounds are lowest for the Ce member. This strongly suggests that the Ce ion is essentially tetravalent (i.e. has no $4f$-derived magnetic moment).[1]

Some reports are available on the thermal expansion of $R_3(Fe, Ti)_{29}$ (R = Ce, Nd, Gd and Tb) and $Ce_3(Fe, Cr)_{29}$ compounds,[13–15] but none on their

magnetostrictive behavior. In the present work, the magnetoelastic properties of the $Y_3Fe_{27.2}Cr_{1.8}$ and $Ce_3Fe_{25}Cr_4$ compounds are studied via thermal expansion and magnetostriction measurements using the strain gauge method.

2. Experimental Method

$Y_3Fe_{27.2}Cr_{1.8}$ and $Ce_3Fe_{25}Cr_4$ compounds were prepared by arc melting of high-purity (at least 99.9%) constituent elements in a water-cooled copper boat. In order to maximize the amount of $R_3(Fe, Cr)_{29}$ phase, the ingots were subsequently annealed in sealed quartz tubes under a protective argon atmosphere at 1373 K (for $Y_3Fe_{27.2}Cr_{1.8}$)[16] and 1200 K (for $Ce_3Fe_{25}Cr_4$)[1] for a period of two weeks and then water-quenched to room temperature. The prepared samples were examined by the analysis of the X-ray diffraction patterns using the Fullprof program. The X-ray diffraction was performed at room temperature by using CuKα radiation with $2\theta = 0.05^\circ$ resolution. The magnetostriction and linear thermal expansion (LTE) measurements were carried out by the standard strain gauge method on disk-shaped samples of 6 mm diameter and 3 mm thickness in magnetic fields up to 1.5 T, and temperatures ranging from 77 K to 500 K. The spontaneous volume magnetostriction ω_s was calculated as $\omega_s = 3[(\Delta l/l)_{\rm exp} - (\Delta l/l)_{\rm lat}]$; where $(\Delta l/l)_{\rm exp}$ $(= (l(T) - l\ (77\ {\rm K}))/l\ (77\ {\rm K}))$ and $(\Delta l/l)_{\rm lat}$ is the lattice contribution that can be obtained from the extrapolation of the paramagnetic regime of the LTE curve, where only the non-magnetic inharmonic phonon contribution is expected. The extrapolation has been performed using the Grüneisen–Debye model, with a Debye temperature of $T_{\rm D} = 450$ K. The magnetostrictions were measured (with an accuracy of 2×10^{-6}) parallel (longitudinal magnetostriction, λ_l) and normal (transverse magnetostriction, λ_t) to the applied field direction, and then anisotropic magnetostriction, $\Delta\lambda = \lambda_l - \lambda_t$, and volume magnetostriction, $\Delta V/V = \lambda_l + 2\lambda_t$, were derived. The temperature dependence of the low-field AC magnetic susceptibility $\chi_{\rm ac}(T)$ of samples were measured between 100 K and 300 K at 333 Hz with an AC magnetic field of 50 $\rm Am^{-1}$ peak value using a Lake-Shore AC susceptometer model 7000. This measurement was performed using fine temperature intervals in order to obtain the critical behaviors.

3. Results and Discussion

The X-ray powder diffraction patterns of the annealed $Y_3Fe_{27.2}Cr_{1.8}$ and $Ce_3Fe_{25}Cr_4$ compounds are presented in Fig. 1. They can be indexed by the monoclinic $Nd_3(Fe, Ti)_{29}$-type structure and space group of A2/m, using Fullprof analysis. The refined pattern factor R_p, the weighted pattern factor R_{wp} and the expected pattern factor $R_{\rm exp}$ for $Y_3Fe_{27.2}Cr_{1.8}$ are 15.61%, 21.93% and 8.51% and for $Ce_3Fe_{25}Cr_4$ are 12.17%, 17.09% and 10.12%, respectively. Results of the Rietveld analysis indicate that the samples are mainly consisting of the related 3:29 phase with the A2/m space group. In addition, some amounts of 1:12 (S.G. I4/mmm), 2:17H (S.G. P6/mmm) and α-Fe (S.G. Im3m) minor phases are also detected.

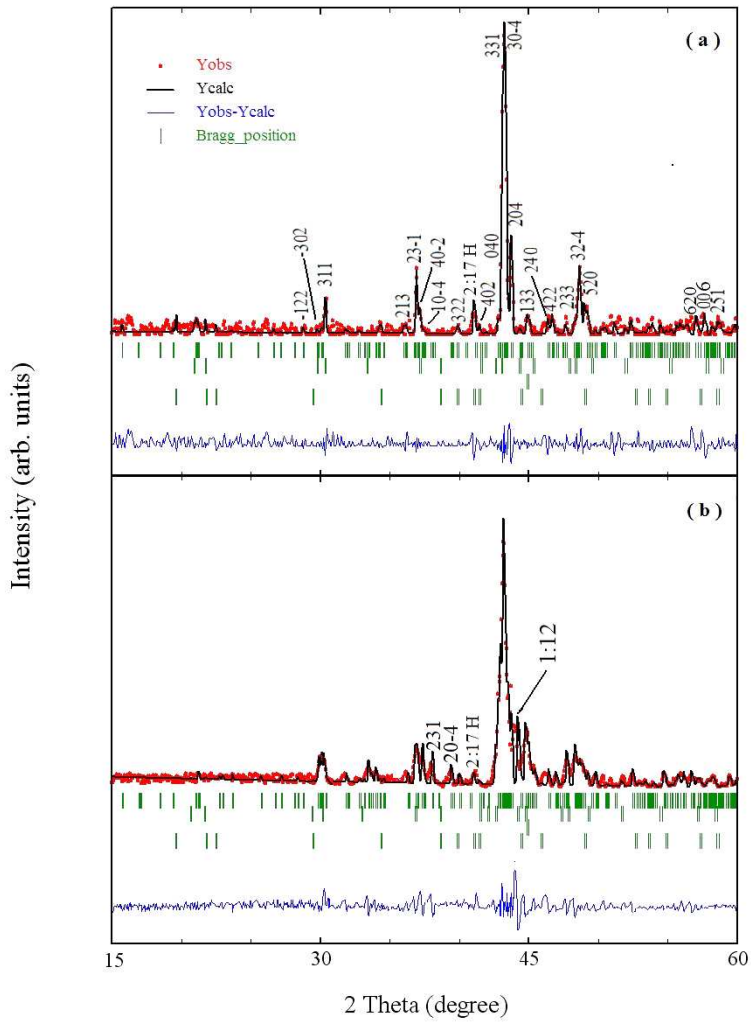

Fig. 1. Rietveld analysis of the X-ray diffraction patterns of (a) $Y_3Fe_{27.2}Cr_{1.8}$ and (b) $Ce_3Fe_{25}Cr_4$ samples. The dots represent the raw data. The solid line represents the calculated profile. Vertical bars indicate the position of Bragg peaks for the 3:29, 1:12, α-Fe and 2:17 structures, respectively. The lowest curve is the difference between the observed and the calculated patterns.

The percentage of these impurities, the lattice constants a, b, c, β and the unit cell volumes V are summarized in Table 1. Traces of α-Fe and 1:12 phases are reported in the other Ce-based compounds as well.[3,6]

The measured linear thermal expansion (LTE) of the samples from 77 K to 500 K, and their calculated linear thermal expansion coefficient, $\alpha(T)$, are displayed in Figs. 2(a) and 2(b), respectively. The well-defined anomalies observed at 427 K and 310 K for $Y_3Fe_{27.2}Cr_{1.8}$ and $Ce_3Fe_{25}Cr_4$ compounds, respectively,

Table 1. Phase composition and unit cell parameters of the $Y_3Fe_{27.2}Cr_{1.8}$ and $Ce_3Fe_{25}Cr_4$ samples.

	Phases	(Wt.%)	a (Å)	b (Å)	c (Å)	β (°)	V (Å^3)
$Y_3Fe_{27.2}Cr_{1.8}$	3:29	93.3	10.568(6)	8.467(3)	9.661(2)	96.953(5)	858.195
	1:12	2.7					
	2:17H	2.3					
	α-Fe	1.7					
$Ce_3Fe_{25}Cr_4$	3:29	90.2	10.523(7)	8.477(9)	9.666(7)	96.703(8)	856.554
	1:12	8.2					
	2:17H	0.5					
	α-Fe	1.1					

are associated with their magnetic phase transitions. The average linear thermal expansion coefficients below magnetic ordering temperatures are approximately 8×10^{-6} and 3×10^{-6} K^{-1} for $Y_3Fe_{27.2}Cr_{1.8}$ and $Ce_3Fe_{25}Cr_4$ compounds, respectively. The LTE of $Ce_3Fe_{25}Cr_4$ compound exhibits an additional anomaly around 216 K with a sharp decrease of $\alpha(T)$. The same anomaly is observed in its low-field AC susceptibility data around 216 K (Fig. 3). The occurrence of a spin re-orientation transition in $R_3(Fe, Ti)_{29}$ single crystals with R = Ce, Pr and Nd (see Ref. 6) and $Ce_3Fe_{25}Cr_4$ compound[3] has not been reported before. However, a spin re-orientation transition has been observed in the $Ce_3Fe_{27.5}Ti_{1.5}$ polycrystalline compound around 210 K.[6] This transition was reported to be due to the presence of a small amount of 1:12 phase in the studied sample. Therefore, one may anticipate that the observed anomaly around 216 K in the thermal expansion and AC susceptibility curves of our $Ce_3Fe_{25}Cr_4$ sample is due to the presence of small amount of $CeFe_{12-x}Cr_x$ phase (1:12 phase) in this sample. As seen in Fig. 2(b), another anomaly is observed at 412 K, which is associated with the magnetic ordering temperature of the secondary phase ($CeFe_{12-x}Cr_x$). This is consistent with the observed anomalous behavior in the thermal expansion curve of the $Ce_3(Fe, Cr)_{29}$ compound.[13] Figure 2(c) shows the temperature dependence of $\omega_s(T)$ for $Y_3Fe_{27.2}Cr_{1.8}$ and $Ce_3Fe_{25}Cr_4$ compounds. It is clear that as the temperature increases from 77 K to T_C, ω_s decreases from 6.7×10^{-3} and 3.5×10^{-3} to near zero for $Y_3Fe_{27.2}Cr_{1.8}$ and $Ce_3Fe_{25}Cr_4$, respectively. The non-zero value of ω_s beyond T_C indicates the existence of strong short-range magnetic correlations similar to other $R_3(Fe, Ti)_{29}$ compounds.[13,17] However, the magnitude of ω_s (77 K) obtained for the $Ce_3Fe_{25}Cr_4$ compound is smaller by a factor three than that reported for $Ce_3Fe_{27.4}Ti_{1.6}$ compound.[17,18] It is well known that the major contribution to ω_s of intermetallic compounds originates from the spontaneous volume magnetostriction of the iron sublattice arising from the exchange interactions between the magnetic moments of the Fe atoms. Therefore, the different values of ω_s in $Ce_3Fe_{25}Cr_4$ and $Ce_3Fe_{27.4}Ti_{1.6}$ compounds can be due to the difference in the average values of Fe magnetic moments in these compounds (1.7 and 1.4 μ_B for the Ti and Cr compounds, respectively[1]). This also indicates that the stabilizing element (M = Cr,

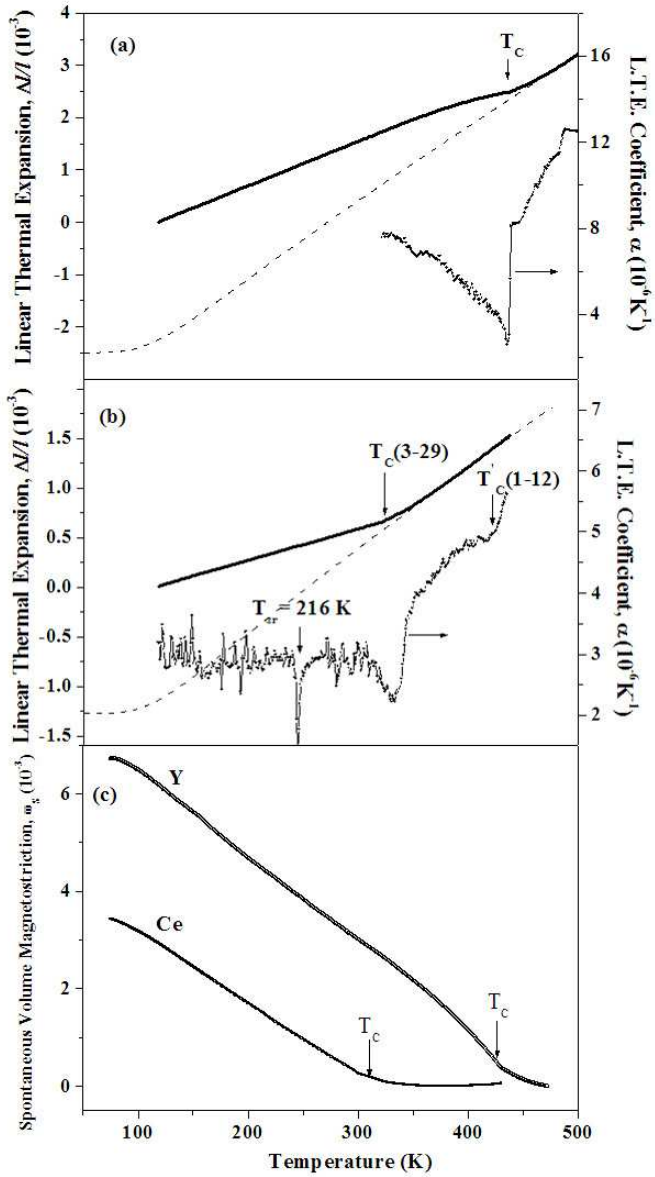

Fig. 2. Temperature dependence of the linear thermal expansion and $\alpha(T)$ of (a) $Y_3Fe_{27.2}Cr_{1.8}$, (b) $Ce_3Fe_{25}Cr_4$ (the dashed lines represent the lattice LTE), and (c) spontaneous volume magnetostriction of the compounds.

Ti . . .) plays a crucial role in the thermal expansion behavior of 3:29 intermetallic system, as in some $RFe_{12-x}M_x$ compounds.[19] It is worth mentioning that the value of unit cell volume of these compounds has influence on the different values and signs of the Fe–Fe exchange interactions.

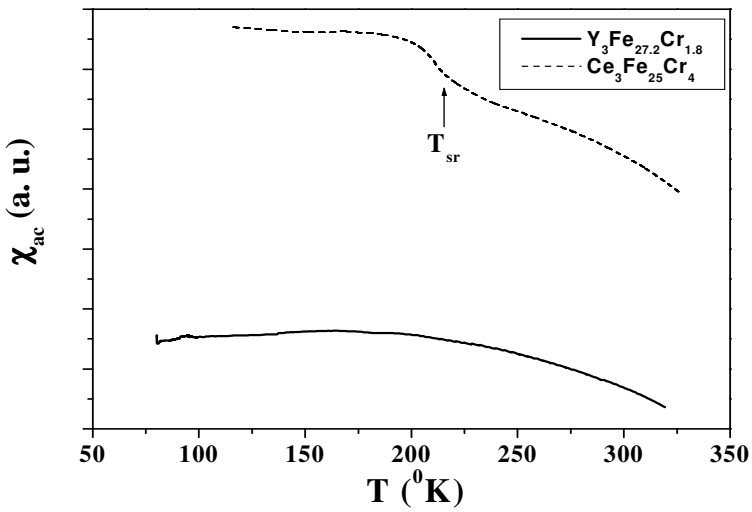

Fig. 3. AC-magnetic susceptibility curves versus temperature for $Y_3Fe_{27.2}Cr_{1.8}$ and $Ce_3Fe_{25}Cr_4$ samples.

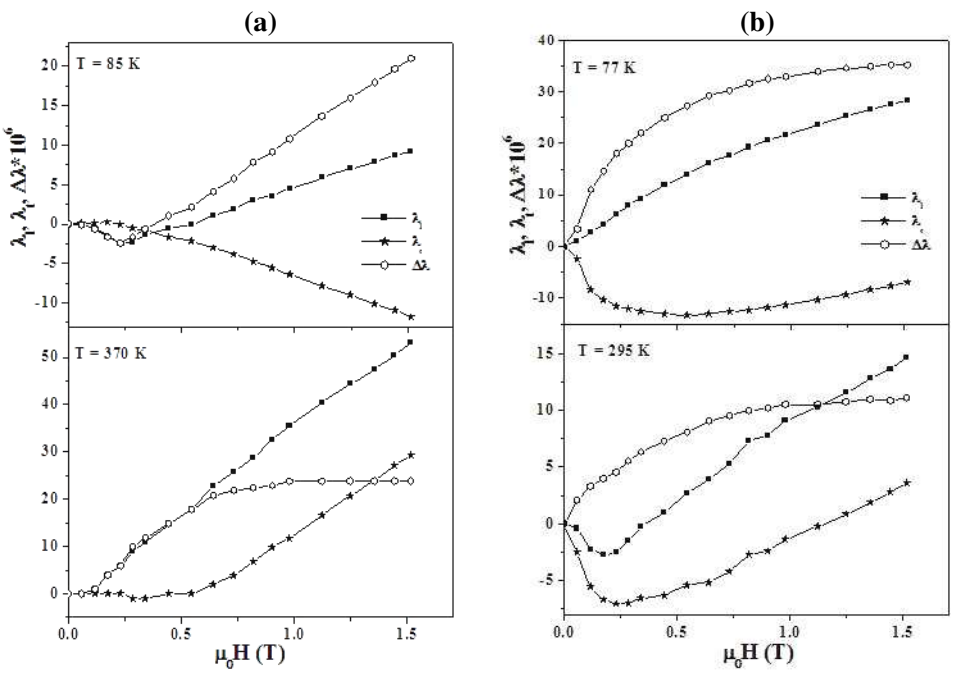

Fig. 4. Isothermal curves of the longitudinal λ_l, transverse λ_t and anisotropic magnetostriction $\Delta\lambda$ of (a) $Y_3Fe_{27.2}Cr_{1.8}$ and (b) $Ce_3Fe_{25}Cr_4$ compounds as a function of applied field at selected temperatures. In this and all the following figures, the lines are guides for the eyes.

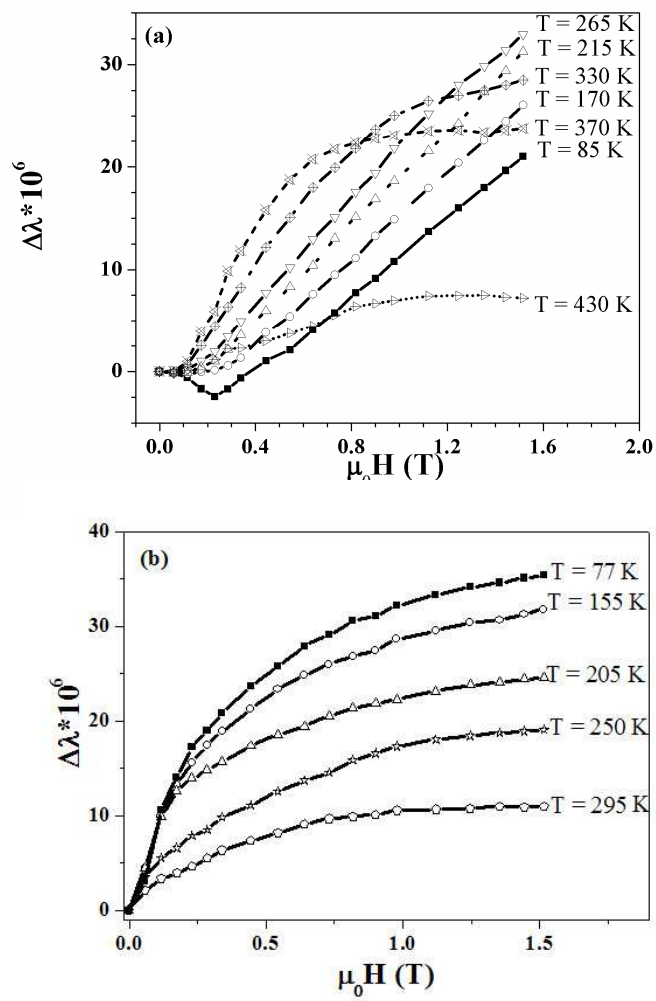

Fig. 5. Isothermal curves of the anisotropic magnetostriction of (a) $Y_3Fe_{27.2}Cr_{1.8}$ and (b) $Ce_3Fe_{25}Cr_4$ samples as a function of applied field at selected temperatures.

The isothermal curves of the longitudinal magnetostriction, λ_l, transverse magnetostriction, λ_t and $\Delta\lambda$ for $Y_3Fe_{27.2}Cr_{1.8}$ and $Ce_3Fe_{25}Cr_4$ samples at selected temperatures are shown in Figs. 4(a) and 4(b). The λ_l and λ_t curves reveal no sign of saturation but the $\Delta\lambda$ curves exhibit saturation type behavior at high temperatures. This is just due to the fact that the values of λ_l and λ_t increase with the same slop when the applied magnetic field is comparable to the anisotropy field.[3]

The isothermal curves of the anisotropic magnetostriction, $\Delta\lambda$, of the samples at some selected temperatures are peresented in Fig. 5. The magnetostriction traces of $Y_3Fe_{27.2}Cr_{1.8}$ exhibit a different behavior to those recorded for $Ce_3Fe_{25}Cr_4$. It is clear that saturation type behavior appears at different temperatures and

applied fields in these compounds. For $Y_3Fe_{27.2}Cr_{1.8}$ an anomalous minimum occurs at low fields and temperatures. The anisotropic magnetostriction curves exhibit a linear variation with a positive slope as temperature increases to about 300 K. The saturation behavior starts from approximately 330 K and continues to beyond the magnetic ordering temperature at 430 K. The value of $\Delta\lambda$ at maximum applied field decreases as saturation begins and reaches a small value at T_C. This is due to the anisotropy field weakness close to the magnetic ordering temperature of the compound.[3] The saturation values of $\Delta\lambda$ deduced by extrapolation of isotherms to $\mu_o H = 0$ T are approximately 23×10^{-6} at 370 K and 5×10^{-6} at 430 K. In the contrary, the anisotropic magnetostriction of the $Ce_3Fe_{25}Cr_4$ compound shows a unique parabolic behavior at all temperatures and tends toward saturation at the high field region as temperature approaches 205 K. The saturation value of $\Delta\lambda$ decreases from 24×10^{-6} at 205 K to approximately 10×10^{-6} at 295 K (near the ordering temperature). The remaining contribution to $\Delta\lambda$ beyond this temperature can be due to the presence of the 1:12 phase in the sample, which is consistence with the $\Delta\lambda$ value of the Fe sublattice in the $YFe_{12-x}V_x$ compounds.[20]

Figure 6 shows the temperature dependence of the anisotropic magnetostriction of the samples in different applied fields of 0.5 T, 1 T and 1.5 T. As is clear that, at all applied fields and temperatures, the $\Delta\lambda$ behavior of $Y_3Fe_{27.2}Cr_{1.8}$ is different from those of $Ce_3Fe_{25}Cr_4$. For $Y_3Fe_{27.2}Cr_{1.8}$, $\Delta\lambda$ at all fields increases up to $T \approx 330$ K, which is due to anisotropic field weakening with temperature, and then decreases to a negligible value around T_C (Fig. 6(a)). The anisotropic magnetostriction curves of $Ce_3Fe_{25}Cr_4$ (Fig. 6(b)) show an anomaly around 216 K, corresponding probably to spin reorientation of the 1:12 phase, and then decrease to limited values at $T_C = 310$ K due to the presence of impurities. The different behavior of the $\Delta\lambda$ curves of $Y_3Fe_{27.2}Cr_{1.8}$ and $Ce_3Fe_{25}Cr_4$ can be attributed to the lower T_C, saturation magnetization, and anisotropy field in the latter compound, due to its less Fe content.[3]

In Fig. 7, the volume magnetostriction ($\Delta V/V$) of the samples is plotted versus the applied field for selected temperatures. In the case of $Y_3Fe_{27.2}Cr_{1.8}$, the $\Delta V/V$ behavior strongly depends on the temperature. The volume magnetostriction is nearly zero in weak fields, and then passes through a minimum at 215 K to 295 K under different applied fields. The curves exhibit parastrictive behavior as temperature rises toward T_C. The easy magnetization direction (EMD) for the isostructural compounds [$R_3(Fe, Ti)_{29}$ (R = Ce, Nd)] is along the a-axis and there is a magnetic anisotropy in the a–b plane of the monoclinic structure.[10,11] In addition, the anisotropy field along the c-axis (H_a^c) is larger than that of the b-axis (H_a^b).[3,10] At low temperatures, where the applied field (H) is smaller than H_a^b and consequently the magnetization vector rotates in the a–b plane, the volume magnetostriction has negative values and increases with the applied field. When $H > H_a^b$, the magnetic moments rotate toward the c-axis and $\Delta V/V$ tends toward the positive values. Finally, when $H > H_a^c$, the magnetization vector rotates toward the applied field resulting in a forced magnetostriction. In the case of $Ce_3Fe_{25}Cr_4$,

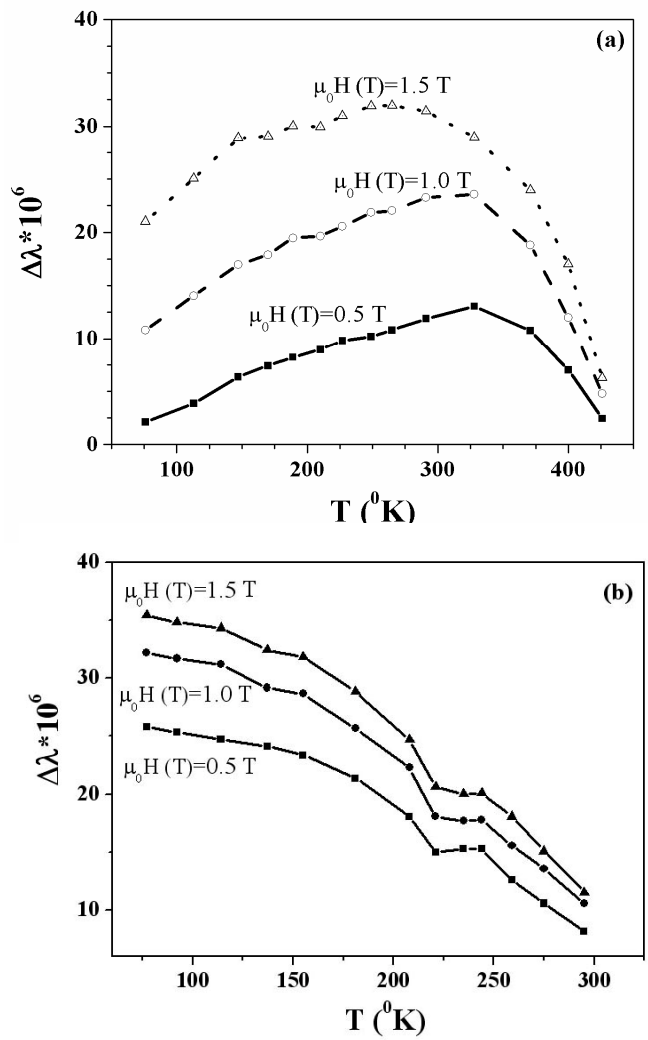

Fig. 6. Temperature dependence of the anisotropic magnetostriction of (a) $Y_3Fe_{27.2}Cr_{1.8}$ and (b) $Ce_3Fe_{25}Cr_4$ compounds at different magnetic fields.

the $\Delta V/V$ behavior is nearly the same, except that the minimum of the curves occur at lower applied fields due to the smaller magnetic anisotropy of $Ce_3Fe_{25}Cr_4$ with respect to that of $Y_3Fe_{27.2}Cr_{1.8}$.[3]

The temperature dependence of the volume magnetostriction of the samples at different applied fields of 0.5 T, 1 T and 1.5 T is shown in Fig. 8. It is clear that $\Delta V/V$ in $Y_3Fe_{27.2}Cr_{1.8}$ has negative values below 270 K, where the magnetic moments are still in the *a*–*b* plane. The same behavior can also be seen for the $Ce_3Fe_{25}Cr_4$ compound in Fig. 8(b). In addition, the anomaly in $\Delta V/V$ curves around 216 K is believed to be due to the presence of the $CeFe_{12-x}Cr_x$ phase (1:12 phase).

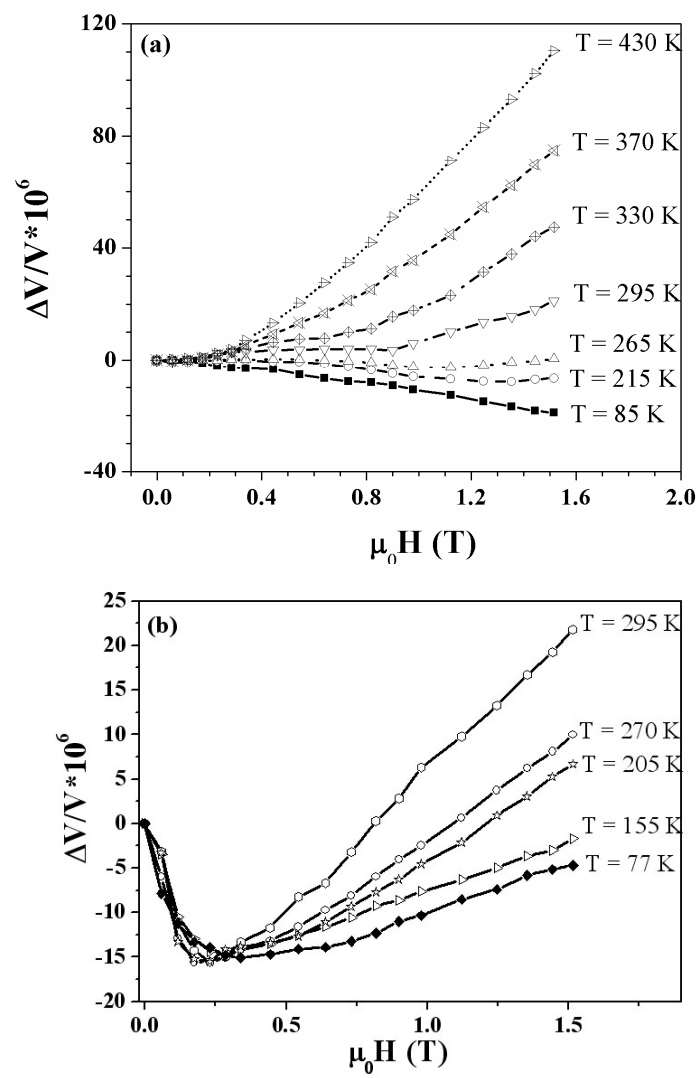

Fig. 7. Isothermal curves of the volume magnetostriction of (a) $Y_3Fe_{27.2}Cr_{1.8}$ and (b) $Ce_3Fe_{25}Cr_4$ samples as a function of applied field at selected temperatures.

4. Conclusion

We investigated the structural and magnetoelastic properties of $Y_3Fe_{27.2}Cr_{1.8}$ and $Ce_3Fe_{25}Cr_4$ ferromagnetic compounds. Rietveld analysis of the X-ray patterns indicates that the main phase of each sample has the $Nd_3Fe_{27.5}Ti_{1.5}$-type structure with monoclinic symmetry. Well defined anomalies are observed in the LTE and $\alpha(T)$ curve of the samples at their Curie temperatures. In $Ce_3Fe_{25}Cr_4$, an additional anomaly is observed around 216 K in $\alpha(T)$ and AC susceptibility curves

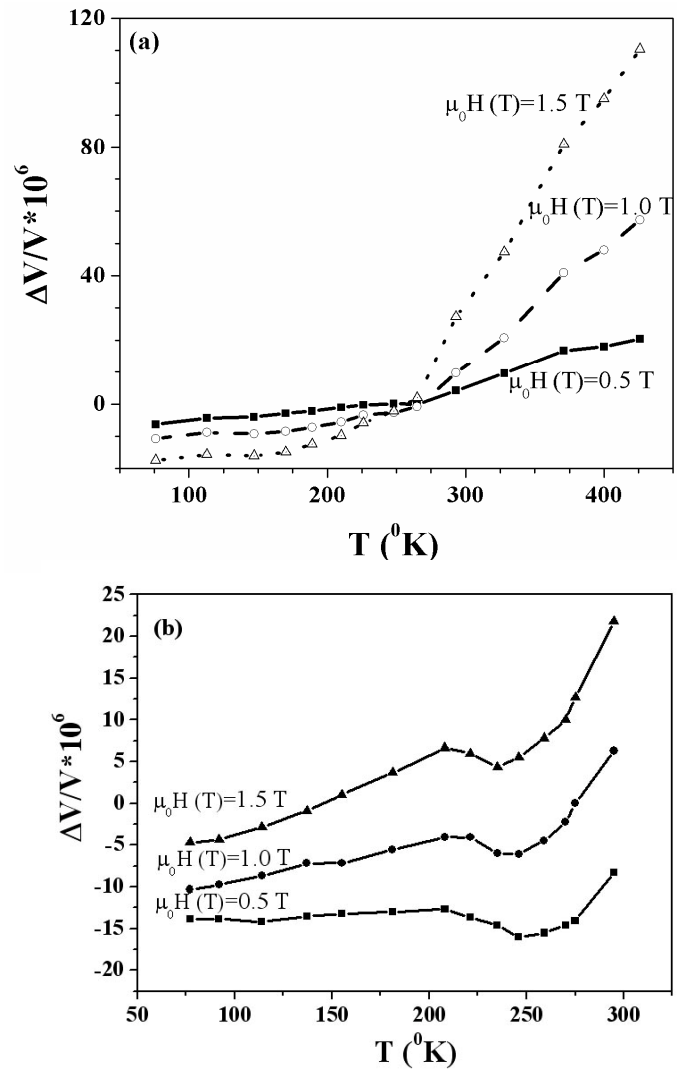

Fig. 8. Temperature dependence of the volume magnetostriction of (a) $Y_3Fe_{27.2}Cr_{1.8}$ and (b) $Ce_3Fe_{25}Cr_4$ compounds at different magnetic fields.

which is probably due to the spin re-orientation of the minor $CeFe_{12-x}Cr_x$ phase (1:12 phase) existing in this sample. For $Y_3Fe_{27.2}Cr_{1.8}$, the saturation behavior is observed in the anisotropic magnetostriction isothermal curves near the magnetic ordering temperature (T_C), whereas for $Ce_3Fe_{25}Cr_4$, a unique parabolic behavior is observed at all temperatures and $\Delta\lambda$ tends towards saturation in the high field region. The volume magnetostriction isotherms of both compounds show sign change in different applied fields and temperatures.

References

1. C. D. Fuerst, F. E. Pinkerton and J. F. Herbst, *J. Appl. Phys.* **76** (1994) 6144.
2. J. M. Cadogan, H.-S. Li, A. Margarian, J. B. Dunlop, D. H. Ryan, S. J. Collocott and R. L. Davis, *J. Appl. Phys.* **76** (1994) 6138.
3. X.-F. Han, F. M. Yang, H. G. Pan, Y. G. Wang, J. L. Wang, H. L. Liu, N. Tang, R. W. Zhao and H. S. Li, *J. Appl. Phys.* **81** (1997) 7450.
4. X.-F. Han, F. M. Yang, H. G. Pan, Y. G. Wang and Y. Z. Wang, *J. Appl. Phys.* **83** (1998) 4366.
5. X.-F. Han, R.-G. Xu, X.-H. Wang, H. G. Pan, T. Miyazaki, J. E. Baggio-Saitovitch, F. M. Yang and C. P. Cheng, *J. Phys. Condens. Matter* **10** (1998) 7037.
6. W. A. Mendoza and S. A. Shaheen, *J. Magn. Magn. Mater.* **195** (1999) 136.
7. L. C. C. M. Nagamine, H. R. Rechenberg, X.-F. Han, E. Baggio-Saitovitch, I. S. Azevedo and L.-Y. Lin, *Phys. Status Solidi B* **221** (2000) 767.
8. X. F. Han, Z. G. Sun, H. Kato, M. Oogane, B. G. Shen, F. M. Yang and J. M. D. Coey, *J. Magn. Magn. Mater.* **239** (2002) 204.
9. O. Kalogirou, V. Psycharis, L. Saettas and D. N. Niarchos, *J. Magn. Magn. Mater.* **146** (1995) 335.
10. V. R. Shah, G. Markandeyulu, K. V. S. Rama Rao, M. Q. Huang, K. Sirisha and M. E. McHenry, *J. Alloys Compd.* **352** (2003) 6.
11. O. Kalogirou, C. Sarafidis, M. Gjoka and G. Litsardakis, *J. Magn. Magn. Mater.* **247** (2002) 34.
12. M. R. Ibarra, L. Morellon, J. Blasco, L. Pareti, P. A. Algarabel, J. Garcoa, F. Albertini, A. Paoluzi and G. Turilli, *J. Phys.: Condens. Matter* **6** (1994) 717.
13. Z. Arnold, J. Kamarad, L. Morellon, P. A. Algarabel, M. R. Ibarra, L. Pareti, F. Albertini, A. Paoluzi and C. D. Furest, *J. Appl. Phys.* **78** (1995) 4615.
14. L. Morellon, P. A. Algarabel, B. Garcia-Landa, M. R. Ibarra, F. Albertini, A. Paoluzi and L. Pareti, *Proc. 8th. Int. Symp. Magnetic Anisotropy and Coercivity in Rare-Earth Transition Metal Alloys*, Birmingham (1994), p. 361.
15. L. Morellon, P. A. Algarabel, M. R. Ibarra, J. Kamarad, Z. Arnold, L. Pareti, F. Albertini and A. Paoluzi, *J. Magn. Magn. Mater.* **150** (1995) L285.
16. H. Z. Luo, L. Jia, Y. X. Li, S. T. Li, J. Shen, N. X. Chen, G. H. Wu and F. M. Yang, *Physica B* **363** (2005) 133.
17. M. R. Ibarra, L. Morellon, J. Blasco, L. Pareti, P. A. Algarabel, J. Garcia, F. Albertini, A. Paoluzi and G. Turilli, *J. Phys. Condens. Matter* **6** (1994) L717.
18. J. Kamarád, Z. Arnold, L. Morellon, P. A. Algarabel, M. R. Ibarra and C. D. Fuerst, *J. Appl. Phys.* **79** (1996) 4656.
19. K. H. J. Buschow, *J. Less-Common Met.* **144** (1988) 65.
20. H. K. Fadafan, N. Tajabor, D. Fruchart and D. Gignoux, *J. Magn. Magn. Mater.* **323** (2011) 988.